

An exact algorithm for spin correlation functions of the two dimensional $\pm J$ Ising spin glass in the ground state

J. Poulter

Department of Mathematics, Faculty of Science, Mahidol University, Rama 6 Road, Bangkok 10400, Thailand

J.A. Blackman

Department of Physics, University of Reading, P.O. Box 220, Reading RG6 6AF, UK

We introduce an exact algorithm for the computation of spin correlation functions for the two dimensional $\pm J$ Ising spin glass in the ground state. Unlike with the transfer matrix method, there is no particular restriction on the shape of the lattice sample, and unlike Monte Carlo based methods it avoids extrapolation from finite temperatures. The computational requirements depend only on the number and distribution of frustrated plaquettes.

PACS numbers: 05.50.q, 64.60.Cn, 75.10.Nr

I. INTRODUCTION

Due to its comparative simplicity, the short range bimodal $\pm J$ Ising system is a widely studied model of a spin glass. The Hamiltonian is of the form proposed by Edwards and Anderson¹

$$H = - \sum_{\langle ij \rangle} J_{ij} \sigma_i \sigma_j \quad (1)$$

where the nearest-neighbor exchange interactions J_{ij} are quenched random variables of fixed magnitude but random sign. These bonds are negative with a probability $p \in [0, 0.5]$ for the square lattice. The canonical model with $p = 0.5$ on the square lattice has been studied the most and it is well accepted that spin glass behavior occurs at zero temperature^{2,3,4,5,6,7}, and persists down to a critical probability p_c of about 0.11^{8,9,10,11,12,13,14,15,16,17,18,19}.

One of the compelling features of the 2-dimensional Ising model is the special property of allowing exact solutions - at least for finite systems in the absence of a magnetic field. A number of authors have taken this approach in various guises^{13,17,20,21,22,23,24,25,26}. One advantage of doing so is that it provides a direct access to the ground state properties without the need to extrapolate from finite temperatures as is necessary, for example, in Monte Carlo based methods.

Good agreement for the values of the ground state energy and entropy is obtained by the various workers. However, to the present, there has been very little development in extending the methodology to a direct calculation of the spin correlations at zero temperature, and most of the results have come from extrapolations from finite temperatures.

The present authors developed an approach^{13,20,21,22}, based on the pfaffian matrix, that appears to capture the essence of the physics of the $\pm J$ system. The algorithm enables certain quantities such as the ground state free energy and entropy to be calculated exactly for very large lattices. The objective of the current paper is to extend

that methodology to give direct access to the zero temperature correlation functions.

Spin correlations for the bimodal Ising spin glass are expected to decay algebraically according to

$$[\langle \sigma_0 \sigma_R \rangle^2]_{av} \sim R^{-\eta} \quad (2)$$

at the critical temperature. In practice, finite size effects dictate that the spin correlations will decay exponentially

$$[\langle \sigma_0 \sigma_R \rangle^2]_{av} \sim R^{-\eta} \exp(-R/\xi) \quad (3)$$

where the correlation length ξ is expected to be proportional to the system size if the latter is large enough.

To our knowledge the only direct computations of spin correlation functions in the ground state are those of Ozeki²⁷. This work used a numerical transfer matrix method with long thin samples of circumference L wrapped around a cylinder of length $9L$ with open ends. The maximum possible circumference for this study was only $L = 12$, a consequence of the transfer matrix computational requirements scaling exponentially with L .

All other attempts to study spin correlations in the ground state have involved extrapolation from finite temperature. Monte Carlo techniques have been employed to obtain results for low temperatures, for example $0.86J$ ²⁸ and $0.63J$ ²⁹. However, it has never been clear just how reliable these extrapolations are.

The transfer matrix method has also been used to obtain spin correlations functions at finite temperature^{14,15,30}, although the sample shape restrictions are severe with cylindrical circumference $L \leq 20$. A better approach is probably the network model¹⁷ where the computational requirements scale as L^3 , not exponentially. Nevertheless, although larger values of L are feasible, the zero temperature limit is inaccessible.

The algorithm we employ depends only on the number and distribution of frustrated plaquettes. This means that there is no need for the cylindrical circumference to

be especially small and the two lattice dimensions can be treated on an essentially equal footing. Although this algorithm is related in some formalities to the network model, it is especially designed to operate in the ground state.

The method is also fully gauge invariant. This means that it is well suited for the determination of gauge invariant quantities. In this context, a transformation of disorder is gauge invariant if the number and distribution of frustrated plaquettes is unchanged. Examples of gauge invariant quantities are energy, entropy and the squares of correlation functions. In contrast, matching algorithms^{24,25,26}, although more efficient, cannot determine more than the energy.

The formalism is developed in Section 2, and is then used in Section 3 for the evaluation of η for the canonical $\pm J$ model.

II. FORMALISM

The planar Ising model has long been analytically accessible since it can be mapped onto a system of non-interacting fermions. This mapping can take various forms, including the transfer matrix and combinatorial methods. The combinatorial, or Pfaffian, method³¹ is particularly well suited to the study of disordered planar Ising systems. Essentially, each lattice site is decorated with four fermions which have interactions across bonds as well as intrasite interactions.

The partition function for a disordered planar Ising model can be expressed in the form

$$Z = 2^N \left[\prod_{\langle ij \rangle} \cosh(J_{ij}/kT) \right] (\det D)^{1/2} \quad (4)$$

where the product is over all nearest neighbor bonds J_{ij} on the N site lattice and D is a skew-symmetric matrix. The square root of the determinant of D is the major feature and is precisely the Pfaffian³¹. It is also proportional to the trace over all closed lattice polygons, that is

$$\text{Tr} \prod_{\langle ij \rangle} (1 + t_{ij} \sigma_i \sigma_j) = 2^{-N} (\det D)^{1/2} \quad (5)$$

where $t_{ij} = \tanh(J_{ij}/kT)$.

The correlation functions can be expressed within the same formalism as a reciprocal defect problem^{20,31}. We choose a path between a pair of spins and replace t_{ij} with t_{ij}^{-1} for bonds on that path. It may be noted here that the path can also be disjoint, in which case the formalism would give a correlation function for four or more spins. In terms of determinants, the correlation function can be easily expressed as

$$\langle \sigma_0 \sigma_R \rangle^2 = \frac{\det C}{\det D} \prod_{\text{path}} t_{ij}^2 \quad (6)$$

where the matrix C is the same as D except for the reciprocal defects.

The calculation of the partition function for the disordered Ising model has been described before²¹. The key points are as follows. At zero temperature, D is a singular matrix with zero eigenvalues equal in number to the number of frustrated plaquettes. These eigenvalues (which occur in pairs) approach zero as some power of $\exp(-2J/kT)$

$$\epsilon = \pm \frac{1}{2} X \exp(-2Jr/kT) \quad (7)$$

where r is an integer. The ground state energy and entropy can be expressed exactly as

$$F = -2J + 2J \sum_d r_d \quad (8)$$

$$S = k \sum_d \ln X_d \quad (9)$$

The sums are over all zero eigenstates. An algorithm based on degenerate state perturbation theory was developed²¹ to evaluate exactly the r and X , and hence the ground state energy and entropy. In this paper we show how to extend this algorithm to the correlation functions as well.

It was found²¹ to be convenient to transform the lattice fermions from the sites to the bonds. In this way, we can associate two fermions with each bond and, on the square lattice, four fermions with each plaquette. Figure 1 provides an illustration. A simple generalization to another planar lattice has proved straightforward²².

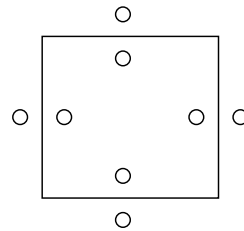


FIG. 1: A plaquette showing how lattice fermions are associated with bonds and plaquettes.

For the $\pm J$ model in particular we write

$$D = D_0 + \delta D_1 \quad (10)$$

where $\delta = 1 - t$ with $t = \tanh(J/kT)$. This equation is exact and D_1 characterizes a perturbation away from the singular matrix D_0 and has nonzero matrix elements only across bonds. The singularities of D_0 arise due to the frustration. For each frustrated plaquette, D_0 has

a zero eigenvalue with an eigenvector localized on the four associated fermions. To determine the ground state properties, it is necessary to determine the defect eigenvalues of D , that is those eigenvalues that are zero at zero temperature. First D_1 is diagonalized in the basis of the defect eigenvectors localized on the frustrated plaquettes. The second order calculation then involves diagonalizing

$$D_2 = D_1 g_c D_1 \quad (11)$$

in the basis of the eigenvectors corresponding to zero eigenvalues at first order. This process is continued order by order where, for $n > 2$,

$$D_n = D_{n-1}(1 + G_{n-2}D_{n-2}) \cdots (1 + G_1 D_1) g_c D_1 \quad (12)$$

until no zero eigenvalues remain. In these equations, g_c is the continuum propagator and G_n is the propagator for eigenstates determined at order n ²¹.

The matrix C is given by

$$C = D_0 + \delta(D_1 + 2V) + (\delta^2 + \delta^3 + \cdots)V \quad (13)$$

where $V = -D_1$ for matrix elements across a path bond. All other elements of V are zero. This equation is easily derived by expanding $t^{-1} - t$ in powers of δ . Since $t^2 = 1$ in the ground state, we can now state our main task as the computation of the limit

$$[\langle \sigma_0 \sigma_R \rangle^2]_{T=0} = \lim_{\delta \rightarrow 0} \frac{\det C}{\det D} \quad (14)$$

To achieve this goal efficiently, we have discovered a remarkable property of the continuum propagator. It can be written as the sum of two terms

$$g_c = g_{c1} + g_{c2} \quad (15)$$

where g_{c1} is 4×4 block diagonal in the four fermions associated within a plaquette and g_{c2} is 2×2 block diagonal in the two fermions associated with a bond. The physical relevance of this decomposition can be realized in that g_{c2} should not play any role in the ground state, being only an issue for excited states. Both g_{c2} and D_1 are bond diagonal, meaning that $g_{c2}D_1$ costs energy while taking us nowhere. We can now state an important theorem concerning the determination of $\det C$.

Theorem. *In the ground state limit, the solution for $\det C$ using*

$$\begin{aligned} C &= D_0 + \delta(D_1 + 2V) + (\delta^2 + \delta^3 + \cdots)V \\ g_c &= g_{c1} + g_{c2} \end{aligned} \quad (16)$$

is exactly the same as the solution using

$$\begin{aligned} C &= D_0 + \delta(D_1 + 2V) \\ g_c &= g_{c1} \end{aligned} \quad (17)$$

Essentially, the effects of g_{c2} exactly cancel the awkward nonlinear terms in δ . We can simply rerun the perturbation theory for $D_1 + 2V$ instead of D_1 , noting that this simply requires a sign change across path bonds. Further, there is an obvious corollary that says that g_{c2} can be simply ignored while computing $\det D$. The continuum propagator is really just g_{c1} and is localized inside plaquettes. The physical sense of this is clear. A proof of the theorem is given in the appendix.

In²¹ it was proven that $\det D$ is proportional to the ground state degeneracy (Equation (9) is an equivalent statement). We can generalize this by considering $\det C$ as proportional to an effective degeneracy for the reciprocal defect system. In fact we can usually write

$$\langle \sigma_0 \sigma_R \rangle^2 = \exp(2(S_C(R) - S_D)) \quad (18)$$

where S_D is the system entropy and S_C is the analog for the reciprocal defect system. This result applies unless the effective energy of the reciprocal defect system is less than the actual energy in which case the correlation function is zero. We are not aware of this result appearing elsewhere in the literature. As a function of system size L , the entropy is expected to vary as¹³

$$S_D(L) = S_{D1} + S_{D2}/L \quad (19)$$

with $S_{D2} > 0$ for $p > p_c$ and $S_{D2} < 0$ otherwise. This same behavior is also expected with cylindrical winding, that is periodic boundary conditions applied in one dimension. From this, we can of course reasonably expect that the first cumulant approximation

$$\langle \sigma_0 \sigma_R \rangle^2 \sim A(R) \exp(-B(R)/L) \quad (20)$$

is valid if L is sufficiently large. This is of course in accordance with finite size scaling theory, where it is expected that $A(R) \sim R^{-\eta}$ and $B(R) \sim R$ if R is sufficiently large. The nature of higher order corrections with cylindrical winding is unclear³².

III. RESULTS

We have first estimated correlation functions with paths of length R , in units of the lattice spacing, parallel to the axes of long thin cylinders of dimensions $9L \times L$ with $L = 12, 16, 32$ and 64 . Ozeki²⁷ used similar geometry, but the largest size treated was $L = 12$. The results are displayed in figure 2. The error bars indicate uncertainties equal to two standard deviations, that is a 95.4 per cent confidence interval. The averages are over 10^5 random samples, except for $L = 64$ where only 10^4 samples were obtained. The uncertainties do not depend strongly on either L or R , only on the number of samples. With 10^5 samples, they all sit in the range 0.0021

to 0.0026. The corresponding interval with 10^4 samples is 0.0073 to 0.0086, about a factor of $\sqrt{10}$ larger. The curves are fits of the data to the form

$$\langle \sigma_0 \sigma_R \rangle^2 = AR^{-\eta} \exp(-R/\xi) \quad (21)$$

These χ^2 nonlinear fits were done using the Levenberg-Marquardt method³³ with the statistical uncertainties incorporated.

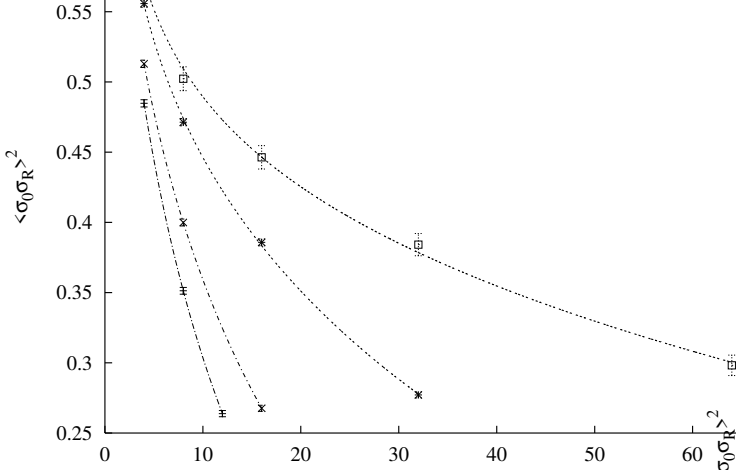


FIG. 2: The square of the spin correlation function on $9L \times L$ lattices with $L = 12$ (pluses), 16 (crosses), 32 (stars) and 64 (squares).

The coefficient A and the exponent η are both approximately independent of L . The values of A are 0.73(4), 0.72(2), 0.72(1) and 0.71(3) respectively for $L = 12, 16, 32$ and 64. The corresponding values of η are 0.12(6), 0.14(3), 0.15(1) and 0.14(2). In comparison, the correlation length ξ does not vary like L as would be expected from finite size scaling theory. In fact we find that it varies more like $L^{3/2}$. The respective values of $\xi/L^{3/2}$ are 0.41(6), 0.41(4), 0.40(3) and 0.47(10). We also find that finite size corrections to the entropy for the $9L \times L$ system scale like $L^{-3/2}$, whereas scaling as equation (19) applies with the $L \times L$ lattice. Clearly the correlation functions are intimately associated with the entropy as is highlighted in equation (18). Interestingly Lukic et al³⁴ also observe finite size corrections to the ground state entropy scaling like $L^{-3/2}$, albeit for a system with different geometry.

Figure 3 shows the same data plotted against $L^{-3/2}$ for $R = 4, 8, 16$ and 32. The χ^2 fits are to the function $\alpha(R) \exp(-\beta(R)L^{-3/2})$ and were first done with linearized data before polishing with nonlinear fits to obtain uncertainties for the fitting parameters $\alpha(R)$ and $\beta(R)$. A consequent fit of $\alpha(R)$ to a power function $R^{-\eta}$ gives $\eta = 0.14(1)$. We have also tried to fit the data to the form of equation (20). The result is certainly inferior with considerably larger χ^2 values for $R = 8$ and 16 in particular, although $B(R)$ does follow R rather roughly. In detail, for $R = 4, 8, 16$ and 32, the respective values of $B(R)/R$ are 0.65(6), 0.69(4), 0.72(4) and 0.65(9).

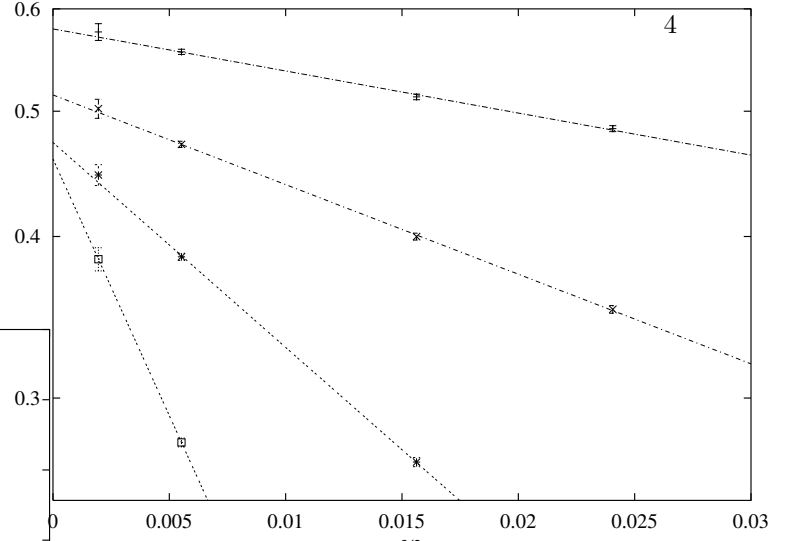


FIG. 3: As figure 2 with the data plotted against $L^{-3/2}$ for $R = 4$ (pluses), 8 (crosses), 16 (stars) and 32 (squares).

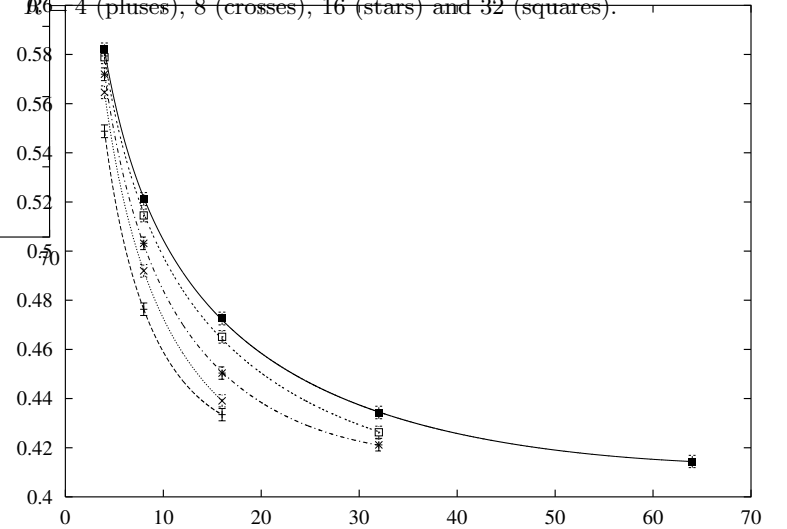


FIG. 4: The square of the spin correlation function on $L \times L$ lattices with $L = 32$ (pluses), 48 (crosses), 64 (stars), 96 (squares) and 128 (filled squares).

We have also performed estimations of correlation functions on $L \times L$ lattices. The lattices are cylindrically wound as before but the reciprocal defect path is around the circumference of the cylinder, as far as possible from the nested boundaries. Figure 4 shows the results for a range of values of L up to 128. The number of random samples taken was 10^5 . The curves are a fit to the form of equation (21) and serve only as a guide to the eye. The statistical uncertainties for our estimates, with 10^5 random samples, on $L \times L$ lattices are in the interval 0.0021 to 0.0026, the same as for the $9L \times L$ lattices.

Figure 5 shows data plotted against L^{-1} . The fits are to the form of equation (20). Only data for which $L > 2R$ is used since it is observed that data for smaller L sits significantly above the fit. This is most probably a consequence of the finite size effect of the cylindrical circumference. A further fit of $A(R)$ to $R^{-\eta}$ reveals $\eta = 0.13(1)$ which is in reasonable agreement with the values found above.

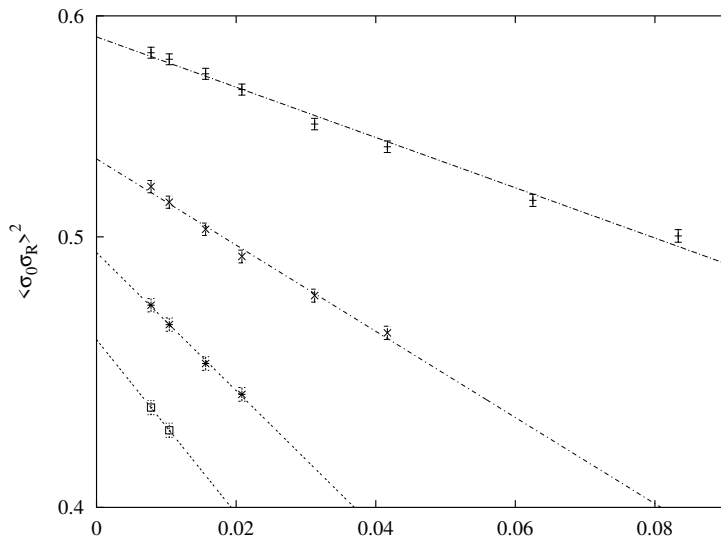


FIG. 5: The square of the spin correlation function on $L \times L$ lattices with $R = 4$ (pluses), 8 (crosses), 16 (stars) and 32 (squares).

IV. DISCUSSION

Earlier work on the exact calculation of the energy and entropy of the 2-dimensional $\pm J$ spin glass has been extended to cover spin correlations in the ground state. The computational requirements of the algorithm depend only on the number and distribution of frustrated plaquettes, and this provides the possibility of studying quite large samples. The big advantage of the approach is that there is no need to extrapolate from finite temperatures as in Monte Carlo methods.

Our best estimate of the exponent is $\eta = 0.14$. We regard the cylindrical winding as the most reliable configuration for calculation since it provides one long dimension. This value for η emerges from the calculation for the largest value of L , and for the composite analysis in Figure 3. The calculation on the $L \times L$ lattice also yields a similar figure.

A wide range of values of η have been reported in the literature over the years. A significant number of these favor a value around 0.2, somewhat higher than ours, but most of these use extrapolated Monte Carlo data rather than focusing directly on the ground state. Interestingly a recent calculation⁷ reports $\eta = 0.138 \pm 0.005$ in agreement with the current calculation.

APPENDIX A

Although the central theorem of this article makes good physical sense, it can also be proven with mathematical rigor. This appendix outlines a proof. For present purposes, all matrices are defined as pure imaginary Hermitian, that is with real eigenvalues.

The main issue is finding the eigenvalues of

$$C = D_0 + \delta(D_1 + 2V) + (\delta^2 + \delta^3 + \dots)V \quad (\text{A1})$$

The eigenvalue equation is formally written

$$C | \Psi \rangle = \lambda | \Psi \rangle \quad (\text{A2})$$

and λ and $| \Psi \rangle$ can be expanded in powers of δ

$$\lambda = \delta^n \epsilon_n^j + O(\delta^{n+1}) \quad (\text{A3})$$

$$| \Psi \rangle = | \Psi_0 \rangle + \delta | \Psi_1 \rangle + \dots \quad (\text{A4})$$

where the eigenvalue is the j th defect eigenvalue of order n with $n > 0$ and $| \Psi_0 \rangle = | n, j \rangle$ is the leading term for the corresponding eigenvector, that is $D_0 | n, j \rangle = 0$. The notation here is in keeping with²¹.

For $1 \leq m \leq n$, equating powers of δ , we obtain

$$D_0 | \Psi_m \rangle + C_1 | \Psi_{m-1} \rangle + V \sum_{p=2}^m | \Psi_{m-p} \rangle = \delta_{mn} \epsilon_n^j | n, j \rangle \quad (\text{A5})$$

where $C_1 = D_1 + 2V$ and the sum vanishes for $m < 2$. From this it follows that

$$\langle r, i | C_1 | \Psi_{m-1} \rangle + \sum_{p=2}^m \langle r, i | V | \Psi_{m-p} \rangle = \delta_{mn} \delta_{rn} \delta_{ij} \epsilon_n^j \quad (\text{A6})$$

Then, for $m = n = r = 1$ we now have

$$\langle 1, i | C_1 | 1, j \rangle = \delta_{ij} \epsilon_1^j \quad (\text{A7})$$

and the first order states are determined by diagonalization of C_1 in the defect basis set, that is the localized vectors associated with the frustrated plaquettes.

Following a development similar to that given for the matrix D in²¹ we can show that

$$| \Psi_m \rangle = g_c C_1 | \Psi_{m-1} \rangle + g_c V \sum_{p=2}^m | \Psi_{m-p} \rangle - \delta_{mn} g_c \epsilon_n^j | n, j \rangle + \sum_{r,i} | r, i \rangle Z_r^i \quad (\text{A8})$$

where Z_r^i is an undetermined coefficient.

For $1 \leq m \leq n-1$, we now use equations (A6) and (A8) to proceed to the second order problem. As stated in the main text, we write $g_c = g_{c1} + g_{c2}$. Further, it is easy to demonstrate that $g_{c2} D_1 = \frac{1}{2}$, $V g_{c2} V = -\frac{1}{2} V$, $C_1 g_{c2} V = -\frac{1}{2} V$ and $C_1 g_{c2} C_1 + V = \frac{1}{2} C_1$. Then, defining $C_2 = C_1 g_{c1} C_1$, it can be shown that, for $r > 1$,

$$\langle r, i | C_2 | \Psi_{m-1} \rangle + \sum_{p=2}^m \langle r, i | C_1 g_{c1} V | \Psi_{m-p} \rangle = \delta_{m,n-1} \delta_{rn} \delta_{ij} \epsilon_n^j \quad (\text{A9})$$

and we can determine the second order states using

$$\langle 2, i | C_2 | 2, j \rangle = \delta_{ij} \epsilon_2^j \quad (\text{A10})$$

Also, with $r = 1$, we can now find the coefficients

$$Z_1^i = -\frac{1}{\epsilon_1^i} \langle 1, i | C_2 | \Psi_{m-1} \rangle - \frac{1}{\epsilon_1^i} \sum_{p=2}^m \langle 1, i | C_1 g_{c1} V | \Psi_{m-p} \rangle \quad (\text{A11})$$

and, with the definition

$$F_r = -\sum_i |r, i\rangle \frac{1}{\epsilon_r^i} \langle r, i |, \quad (\text{A12})$$

we find that

$$|\Psi_m\rangle = ((1 + F_1 C_1) g_{c1} + g_{c2}) \times \left(C_1 | \Psi_{m-1} \rangle + V \sum_{p=2}^m | \Psi_{m-p} \rangle \right) + \sum_{r>1, i} |r, i\rangle Z_r^i \quad (\text{A13})$$

Note that we are using F_r for the propagators of the system with reciprocal defects to avoid confusion with the G_r used in²¹ for the diagonalisation of D .

Next we consider $1 \leq m \leq n - 2$ and work with equations (A9) and (A13) as well as the results $C_2 g_{c2} V = -\frac{1}{2} C_1 g_{c1} V$ and $C_2 g_{c2} C_1 = \frac{1}{2} C_2 - C_1 g_{c1} V$. We also define $C_3 = C_2(1 + F_1 C_1) g_{c1} C_1$. Then, for $r > 2$, we can arrive at

$$\langle r, i | C_3 | \Psi_{m-1} \rangle + \sum_{p=2}^m \langle r, i | C_2(1 + F_1 C_1) g_{c1} V | \Psi_{m-p} \rangle = \delta_{m, n-2} \delta_{rn} \delta_{ij} \epsilon_n^j \quad (\text{A14})$$

Clearly the third order problem is solved by diagonalizing C_3 . Furthermore, for $r = 2$, it is possible to determine the coefficients Z_2^i and we find that

$$|\Psi_m\rangle = ((1 + F_2 C_2)(1 + F_1 C_1) g_{c1} + g_{c2}) \times \left(C_1 | \Psi_{m-1} \rangle + V \sum_{p=2}^m | \Psi_{m-p} \rangle \right) + \sum_{r>2, i} |r, i\rangle Z_r^i \quad (\text{A15})$$

To prove the main result, we can use induction. First we define, for $k \geq 3$,

$$C_k = C_{k-1}(1 + F_{k-2} C_{k-2}) \cdots (1 + F_1 C_1) g_{c1} C_1 \quad (\text{A16})$$

and, for $1 \leq m \leq n - k + 1$ and $r \geq k - 1$, introduce two assumptions. First,

$$\begin{aligned} & \langle r, i | C_k | \Psi_{m-1} \rangle + \\ & \sum_{p=2}^m \langle r, i | C_{k-1}(1 + F_{k-2} C_{k-2}) \cdots (1 + F_1 C_1) g_{c1} V | \Psi_{m-p} \rangle \\ & = \delta_{m, n-k+1} \delta_{rn} \delta_{ij} \epsilon_n^j \end{aligned} \quad (\text{A17})$$

and, second

$$\begin{aligned} & | \Psi_m \rangle = ((1 + F_{k-1} C_{k-1}) \cdots (1 + F_1 C_1) g_{c1} + g_{c2}) \\ & \times \left(C_1 | \Psi_{m-1} \rangle + V \sum_{p=2}^m | \Psi_{m-p} \rangle \right) + \sum_{r \geq k, i} |r, i\rangle Z_r^i \end{aligned} \quad (\text{A18})$$

We can note that, comparing with equations (A14) and (A15), these assumptions are both true for $k = 3$. Also, with the definition (A16), we can easily show that

$$C_k g_{c2} V = -\frac{1}{2} C_{k-1}(1 + F_{k-2} C_{k-2}) \cdots (1 + F_1 C_1) g_{c1} V \quad (\text{A19})$$

and

$$C_k g_{c2} C_1 = \frac{1}{2} C_k - C_{k-1}(1 + F_{k-2} C_{k-2}) \cdots (1 + F_1 C_1) g_{c1} V \quad (\text{A20})$$

Now, for $1 \leq m \leq n - k$ and $r \geq k$, we can use the assumptions (A17) and (A18) with (A19) and (A20) to prove two results. First, for $r > k$,

$$\begin{aligned} & \langle r, i | C_{k+1} | \Psi_{m-1} \rangle + \\ & \sum_{p=2}^m \langle r, i | C_k(1 + F_{k-1} C_{k-1}) \cdots (1 + F_1 C_1) g_{c1} V | \Psi_{m-p} \rangle \\ & = \delta_{m, n-k} \delta_{rn} \delta_{ij} \epsilon_n^j \end{aligned} \quad (\text{A21})$$

and, second, after determining the coefficients Z_k^i ,

$$\begin{aligned} & | \Psi_m \rangle = ((1 + F_k C_k) \cdots (1 + F_1 C_1) g_{c1} + g_{c2}) \\ & \times \left(C_1 | \Psi_{m-1} \rangle + V \sum_{p=2}^m | \Psi_{m-p} \rangle \right) \\ & + \sum_{r>k, i} |r, i\rangle Z_r^i \end{aligned} \quad (\text{A22})$$

This completes the proof of the theorem. Clearly the assumptions (A17) and (A18) imply the results (A21) and (A22). The eigenvalues of C are determined by diagonalisations of the C_r which are defined independently of g_{c2} .

-
- ¹ S.F. Edwards and P.W. Anderson, *J. Phys. F: Met. Phys.* **5**, 965 (1975).
 - ² N. Kawashima and H. Rieger, *Europhys. Lett.* **39**, 85 (1997).
 - ³ H. Kitatani and A. Sinada, *J. Phys. A: Math. Gen.* **33**, 3545 (2000).
 - ⁴ A.K. Hartmann and A.P. Young, *Phys. Rev. B* **64**, 180404(R) (2001).
 - ⁵ J. Houdayer, *Eur. Phys. J. B* **22**, 479 (2001).
 - ⁶ R. Sungthong and J. Poulter, *J. Phys. A: Math. Gen.* **36**, 6347 (2003).
 - ⁷ H.G. Katzgraber and L.W. Lee, *cond-mat/0411305* (2004).
 - ⁸ S. Kirkpatrick, *Phys. Rev. B* **16**, 4630 (1977).
 - ⁹ I. Morgenstern and K. Binder, *Phys. Rev. B* **22**, 288 (1980).
 - ¹⁰ Y. Ozeki and H. Nishimori, *J. Phys. Soc. Japan* **56**, 3265 (1987).
 - ¹¹ H. Kitatani and T. Oguchi, *J. Phys. Soc. Japan* **59**, 3823 (1990).
 - ¹² Y. Ueno and Y. Ozeki, *J. Stat. Phys.* **64**, 227 (1991).
 - ¹³ J.A. Blackman, J. R. Gonçalves, and J. Poulter, *Phys. Rev. E* **58**, 1502 (1998).
 - ¹⁴ F.D.A. Aarao Reis, S.L.A. de Queiroz, and R.R. dos Santos, *Phys. Rev. B* **60**, 6740 (1999).
 - ¹⁵ A. Honecker, M. Picco, and P. Pujol, *Phys. Rev. Lett.* **87**, 047201 (2001).
 - ¹⁶ F.D. Nobre, *Phys. Rev. E* **64**, 046108 (2001).
 - ¹⁷ F. Merz and J.T. Chalker, *Phys. Rev. B* **65**, 054425 (2002).
 - ¹⁸ H. Nishimori and K. Nemoto, *J. Phys. Soc. Japan* **71**, 1198 (2002).
 - ¹⁹ C. Amoruso and A.K. Hartmann, *Phys. Rev. B* **70**, 134425 (2004).
 - ²⁰ J.A. Blackman, *Phys. Rev. B* **26**, 4987 (1982).
 - ²¹ J.A. Blackman and J. Poulter, *Phys. Rev. B* **44**, 4374 (1991).
 - ²² J. Poulter and J.A. Blackman, *J. Phys. A: Math. Gen.* **34**, 7527 (2001).
 - ²³ L. Saul and M. Kardar, *Phys. Rev. E* **48**, R3221 (1993); *Nucl. Phys. B* **432**, 641 (1994).
 - ²⁴ F. Barahona, R. Maynard, R. Rammal, and J.P. Uhry, *J. Phys. A: Math. Gen.* **15**, 673 (1982).
 - ²⁵ U. Derigs and A. Metz, *Math. Program* **50**, 113 (1991).
 - ²⁶ R.G. Palmer and J. Adler, *Int. J. Mod. Phys. C* **10**, 667 (1999).
 - ²⁷ Y. Ozeki, *J. Phys. Soc. Japan* **59**, 3531 (1990).
 - ²⁸ W.L. McMillan, *Phys. Rev. B* **28**, 5216 (1983).
 - ²⁹ J.-S. Wang and R.H. Swendsen, *Phys. Rev. B* **37**, 7745 (1988); *Phys. Rev. B* **38**, 4840 (1988); *cond-mat/0407273* (2004).
 - ³⁰ S.L.A. de Queiroz and R.B. Stinchcombe, *Phys. Rev. B* **68**, 144414 (2003).
 - ³¹ H.S. Green and C.A. Hurst, *Order-Disorder Phenomena* (Interscience, London, 1964).
 - ³² I.A. Campbell, A.K. Hartmann, and H.G. Katzgraber, *Phys. Rev. B* **70**, 054429 (2004).
 - ³³ W.H. Press, S.A. Teukolsky, W.T. Vetterling, and B.P. Flannery, *Numerical Recipes in Fortran* (Cambridge University Press, 1992).
 - ³⁴ J. Lukic, A. Galluccio, E. Marinari, O.C. Martin, and G. Rinaldi, *Phys. Rev. Lett.* **92**, 117202 (2004).